Accepted Manuscript

An Asymmetric Elastic-Plastic Analysis of the Load-Controlled Rotating Bending Test and Its Application in the Fatigue Life Estimation of Wrought Magnesium AZ31B

E. Kalatehmollaei, H. Mahmoudi-Asl, H. Jahed

PII: S0142-1123(14)00061-9
DOI: http://dx.doi.org/10.1016/j.ijfatigue.2014.02.012
Reference: JIJF 3323

To appear in: *International Journal of Fatigue*

Received Date: 11 September 2013
Revised Date: 7 February 2014
Accepted Date: 13 February 2014

Please cite this article as: Kalatehmollaei, E., Mahmoudi-Asl, H., Jahed, H., An Asymmetric Elastic-Plastic Analysis of the Load-Controlled Rotating Bending Test and Its Application in the Fatigue Life Estimation of Wrought Magnesium AZ31B, *International Journal of Fatigue* (2014), doi: http://dx.doi.org/10.1016/j.ijfatigue.2014.02.012

An Asymmetric Elastic-Plastic Analysis of the Load-Controlled Rotating Bending Test and Its Application in the Fatigue Life Estimation of Wrought Magnesium AZ31B

Kalatehmollaei, E; Mahmoudi-Asl, H; Jahed, H[1]

Mechanical and Mechatronics Engineering Department, University of Waterloo, Waterloo, CANADA

Abstract

Due to different deformation mechanisms arising from limited slip systems in HCP wrought magnesium alloys, their yield and hardening in tension and compression are different. Consequently, the cyclic behavior of these alloys is asymmetric showing a non-Masing hysteresis. An elastic-plastic method of analysis is proposed in this paper to handle the pronounced asymmetry inherited by Mg wrought alloys. Samples machined from an extrusion piece of AZ31B were tested on a standard rotating bending machine at bending moment amplitudes ranging from 3.3 to 6.3 N·m. Tests were conducted under two conditions: as-extruded and stress-relived. As-extruded samples showed a higher fatigue limit due to beneficial residual stresses induced by the extrusion process. The proposed elastic-plastic model was then applied to obtain the stress distribution in the tested specimens. Cyclic hystereses obtained from this analysis were used to estimate the elastic and plastic strain energy densities per cycle. An energy-life model for AZ31B was then employed in conjunction with the calculated hysteresis energies to predict fatigue life of AZ31B in rotating bending. The proposed model prediction results were in good agreement with the experimental results.

Keywors: Rotating Bending Test, Magnesium Alloys, Elastic-Plastic Analysis, Fatigue Life

1. Introduction

Recently there has been growing interest in the use of magnesium alloys as material for automotive parts because of their low weight. Magnesium alloys are the lightest commercial alloys and have high specific strength and excellent machinability. Wrought magnesium alloys in particular have been demonstrated to be good candidates to replace other metals in load-bearing automotive components. Since most load-bearing components in automobiles are subject to fluctuating loads, magnesium's fatigue behavior needs to be properly assessed. A recent review on the progress in fatigue behavior of magnesium research can be found in Mirza and Chen [1].

The Rotating Bending Test (RBT) is a standard test adopted by industries worldwide. The main difference between RBT and other servo hydraulic uniaxial load, stress, and strain controlled tests is the non-uniformity of stress at sections within the gauge length. In RBT, the gradient of stress across the gauge section results in plastic deformation near the surface, which is surrounded by the elastic

[1] Corresponding author, Hamid Jahed, 200 University Avenue West, Waterloo, Ontario, N2L5H5, CANADA; Phone: +15198884567x37826; email: hjahed@uwaterloo.ca

core at high bending loads. To obtain the stress induced by the applied bending load, an elastic-plastic analysis is required.

A key tool for the fatigue modeling of automotive components is knowledge of their cyclic behavior. It is well established that wrought magnesium alloys have directional anisotropy; this leads to yield and hardening asymmetry of the material [2, 3]. Such behaviors are related to the hexagonal close-packed shape crystals and the limited slip systems characteristic of wrought magnesium alloys. The asymmetry of these alloys is also the result of twinning deformation that depends on the direction of loading with respect to the crystals arrangement [4]. The yield and hardening asymmetry of magnesium alloys results in asymmetric hysteresis and non-Masing behavior. The asymmetric hysteresis and the deformation mechanisms associated with it within one cycle of loading have been summarized schematically by Albinmousa [2] and are also reproduced here (Figure 1). The figure depicts the cyclic behavior of an AZ31B extrusion sample that was cut along the extrusion direction; the c-axis is therefore perpendicular to the loading direction. The yielding in the first reversal in the tension is caused by slip (point 1-2). Upon unloading from the tension and at the beginning of the second reversal, elastic unloading takes place (point 2-3), until deformation twinning due to extension twins along the c-axis causes plasticity (point 3-4). The third reversal starts with de-twinning (point 4-5). The well-known sigmoidal shape of the curve in the third reversal is due to de-twinning. At the end of this reversal, yielding occurs due to the slip. The asymmetric behavior of AZ31B makes it difficult to predict its response to cyclic loading, such as the loading that would be incurred under rotating bending. Any successful modeling of cyclic behaviour of AZ31B should include the features shown in Figure 1.

Figure 1. Typical cyclic behaviour of magnesium alloy AZ31B extrusion within one cycle of loading [2]

Only a few researchers have reported the load- and stress-controlled cyclic response of AZ31B. Nan et al. [4] reported the fatigue behavior of AZ31B under the cantilever-type RBT. They observed a sharp transition from low-cycle fatigue ($<10^5$ cycles) to high-cycle fatigue. The fatigue life increased from 10^5 cycles under 122.5 MPa of stress to $5x10^7$ cycles under 120MPa of stress; showing the flatness of the stress life curve close to 120MPa. The endurance limit was reported to be close to 120 MPa. Hasegawa et al. [5] performed stress- and strain-controlled cyclic tests on AZ31B and reported that the cyclic response in stress-controlled tests is different from the response in strain-controlled tests. They attributed this difference to different deformation mechanisms of AZ31B. The critical resolved shear required to cause twinning in compression is much lower than the stress required to cause a basal slip in tension. Hence, the compressive strains in fully-reversed stress-controlled tests are up to an order of magnitude larger than the tensile strains in the first few cycles. The half-life cycle bears a mean strain. They suggested that the Coffin-Manson fatigue relation is not suitable for fatigue representation of AZ31B in stress-controlled tests. Yin et al. [6] examined the hysteresis loop in plastic strain-controlled fatigue tests on AZ31B. They reported significant differences in the stress amplitudes resulting from tension and compression.

Albinmousa et al. [2, 3, 7] studied the cyclic behavior of AZ31B under uniaxial and multiaxial loads. They reported significant yield and hardening asymmetry of AZ31B, resulting from different deformation mechanisms under tension and compression. They argued that a scalar-valued energy parameter bypasses the ambiguity arising from directional anisotropy and yield asymmetry of AZ31B, which makes it difficult to develop appropriate stress and strain parameter. With this idea in mind, they proposed an energy-based fatigue parameter and showed that it correlates very well with

the fatigue data. Park et al. [8] studied the behavior of the extruded AZ31B under strain- and stress-controlled tests, under a wide range of strain and stress values. By applying stress-, strain-, and energy-based fatigue parameters, they showed that the stress parameter and the strain parameter varied significantly over the life of the alloy,however, the strain energy density remained constant. They attributed the variation of stress and strain amplitudes to the anisotropy and asymmetry of AZ31B and concluded that energy is a suitable fatigue parameter. Shiozawa et al. [9] performed stress- and strain-controlled tests on AZ31B. Similarly to Park et al. [8], they showed that an energy-based fatigue parameter shows a very good correlation with the experimental results. Kwon et al. [10] performed strain-controlled tests on AZ31B and compared the hystereses of compressive and tensile first reversals. They attributed the difference in hystereses to the twinning that occurs in compression. They argued that the Coffin-Manson parameters are insufficient to explain fatigue damage due to twinning, and proposed the use of a parameter that takes both stress and strain into account. Hence, they used strain energy density per cycle as the fatigue parameter. This showed that it remains constant throughout the life over a wide range of strain and stress amplitudes. Most of the above mentioned studies focused on the low cycle fatigue regime.

In the present study, a four-point RBT was performed on samples machined from an extrusion piece of AZ31B in the extrusion direction. The role of the initial residual stresses resulting from the extrusion process on fatigue life is discussed. A simple method is proposed for elastic-plastic analysis of specimens in the RBT. This method is based on the Variable Material Properties (VMP) method of Jahed and Dubey [11]. The method uses the cyclic stress-strain curves to find the stress response of a load-controlled test for a material with asymmetric properties. The application of this method to find the stress response of a magnesium AZ31B specimen under the rotating beam test condition is presented. Available AZ31B fatigue test data from various research labs have been integrated to yield a set of energy-based fatigue parameters that can be applied to model life in low- and- high cycle fatigue regimes. The energy model is then used to estimate the fatigue life in the RBT. The predicted results are compared with the experimental results.

2. Materials and tests

The material used in present study is magnesium alloy AZ31B extrusion. The air-quenched section of the AZ31B extrusion was manufactured by Timminco. This section was extruded from a billet which was 177.8mm in diameter, 406.4 mm in length and had an extrusion ratio of 6. The extrusion temperature was between 360°C and 382°C, and the extrusion exit speed was 50.8 mm/s. The composition of the alloy is presented in Table 1.

Table 1. Composition of the AZ31B extrusion

Al	Mn	Zn	Fe	Ni	Cu
3.10	0.54	1.05	0.0035	0.0007	0.0008

The behavior of the specimen under the monotonic and cyclic loadings applied in this research was reported by Albinmousa et al. [2]. The hysteresis curves of cyclic uniaxial loading of the AZ31B alloy along the extrusion direction are reported by Albinmousa et al. [12]; these curves for a wide range of strain values are shown in Figure 2. The figure depicts the asymmetric behavior of AZ31B, especially in the larger plastic ranges.

Figure 2. Hysteresis curves of AZ31B under cyclic uniaxial loading; a) 0.2%-0.6% and b) 0.7%-2% [12]

All the RBT samples were machined from the extrusion piece along the extrusion direction. The geometry of the specimen used in the RBT is given in Figure 3. Two sets of specimens were tested. The first set was tested in as-received condition after machining. There is an initial compressive residual stress in as-received specimens due to the extrusion process. X-ray diffraction (XRD) stress measurement of the cylindrical specimen in the hourglass zone shows that the compressive stress is 43±1 MPa at the surface. The second set of samples was stress-relieved before RBT. The stress relief process was performed to free residual stresses that were induced by the extrusion process. The ASM-recommended stress relief process (260°C for 15 minutes) has been used for these specimens [13]. The purpose was to evaluate the fatigue strength in absence of any residual stress. XRD measurements on stress-relieved cylindrical specimens in the hourglass area showed that compressive residual stresses at the surface were eliminated.

Figure 3: Round rotating bending specimens of AZ31B

As-received and stress-relieved cylindrical specimens have been tested under rotating bending to generate the S-N curves. All tests were performed under standard laboratory conditions. Tests were performed at frequencies ranging from 50 Hz (for low cycle tests) to 100 Hz (for high cycle tests). Figure 4 shows the S-N curve for the two groups of specimens. The stress values shown are nominal stresses at the gauge section and were calculated from the applied bending moment using the elastic flexural formula.

Except for lives less than 30 000 cycles, the lives of stress-relieved samples are lower than those of as-extruded samples. At a stress level of 120 MPa, the life of the as-extruded sample is an order of magnitude higher than that of the stress-relieved sample, and the fatigue strength of the as-extruded sample is 116 MPa which is 15% higher than that of the stress-relieved sample. This difference can be attributed to the residual stress induced by the extrusion process. The original section was extruded from a billet with a diameter of 178 mm at a temperature between 360 and 380^{o}C. The difference in the cooling rate from the extrusion piece surface to the core has induced beneficial residual stress, leading to life extension.

Figure 4. S-N curves of as-received and stress-relieved specimens of AZ31B

3. Energy-based fatigue model for AZ31B

Various researchers have proposed energy as a suitable parameter to correlate and estimate the fatigue life of magnesium [3, 7, 8, 10, 14, 15]. Most of these studies focused on the low cycle fatigue regime. Using the fatigue data reported by Albinmousa et al. [2, 3], a set of energy-based fatigue parameters are introduced in this study which cover both low- and high-cycle fatigue regimes. Following the method proposed by Jahed and Varvani [16], a Coffin-Manson type of relation is established by using energy-based fatigue parameters and total strain energy density. Figure 5 shows the total energy

versus the life curve for AZ31B over a range of fatigue lives. Also shown are fatigue values reported in the literature [7, 8, 10, 15, 14]. It is evident that the total energy-life curve correlates fatigue data very well in both low and high cycle fatigue regimes.

Figure 5. Total energy-life curve for AZ31B

To calculate the total energy, the plastic and positive elastic energies are considered. The plastic energy is associated with the area inside the hysteresis loop, which represents the energy dissipated due to the plastic work in each cycle (Figure 6). The positive elastic energy (Figure 6), which is defined based on maximum stress, has two roles: firstly, it accounts for the positive mean stress; and secondly, for high cycle regimes in which the range of plastic strains is small and the area inside of the hysteresis is almost zero, it provides the required fatigue damage parameter. The plastic and positive elastic energy ranges are illustrated in Figure 6. The total energy relationship is shown in Equation 1. In this relationship, ΔW_T is the total energy, ΔW_p is the plastic energy, and ΔW_{e+} is the positive elastic energy.

Figure 6. Positive elastic and plastic energy in a hysteresis curve

$$\Delta W_T = \Delta Wp + \Delta W_{e+} \qquad \text{Equation 1}$$

The total energy range is then used in Equation 2 to estimate fatigue life of the AZ31B specimen. In this equation, ΔW_T is the total the energy range, N_f is the number of cycles to failure and W_f, E_f, b, and c are the coefficients, which are related to the material's cyclic characteristics in low- and high-cycle regimes. These coefficients are calculated for AZ31B based on results reported by Albinmousa et al. [2, 3] shown in Table 2.

$$\Delta W_T = W_f\left(N_f\right)^c + E_f\left(N_f\right)^b \qquad \text{Equation 2}$$

Table 2. Energy-based fatigue parameters for AZ31B

Elastic Part- high cycle	**E_f**	**5**
	b	**-0.278**
Plastic Part- low cycle	**W_f**	**190**
	c	**-0.848**

4. Elastic-Plastic Method of Analysis

RBT is a universally known method for determining the fatigue characteristics of materials. In this test, a round specimen, similar to the one shown in Figure 7, rotates along its axis. Meanwhile, a constant load is applied as a bending moment, or two equal concentrated forces, in a four-point bending manner. As the specimen rotates, the material points on its surface are exposed to a fluctuating load from zero (when the point is located on the horizontal plan) to a maximum value (when the point is on the vertical plan). The fluctuating load applied to the specimen causes fatigue failure, which is represented by the number of cycles (N_f) or the number of reversals ($2N_f$) to failure, to a specified percent of drop in load, or to the initiation of a crack on the surface.

Figure 7. Schematic of the loading of a specimen in RBT

In this study, an alternative way to look at the RBT is considered. Instead of a specimen rotating with a stationary load, the specimen is fixed and the load is fluctuated between a maximum and minimum value continuously. In both tests, the gradient of stress and the ranges of stress and strain are very close. However, during a full cycle of loading in RBT, each point on the surface of the specimen is subjected to the maximum/minimum stress twice per cycle. As a result, crack initiation will occur on the weakest point on the surface. However, in the fixed beam with an alternating load, the failure occurs at the top or bottom of the beam, which may or may not be the weakest point on the surface. This may be one of the main reasons for the lower fatigue life in RBT as compared to that under a fluctuating load. Hassan and Liu [17] compared RBT with a fixed beam with alternating loads, and cantilever-type RBTs. They showed that in general, maximum stress occuring in RBTs is higher than that of a fixed beam with alternating stresses, leading to higher strain ranges in RBT. The larger strain and stress in RBT causes higher energy dissipation during one cycle of loading. Such differences in hysteresis curves lead to a lower fatigue strength in the RBT specimen [17]. The method presented here is for elastic-plastic analysis of the fixed beam with a fluctuating load.

The proposed elastic-plastic method of analysis is based on the composite beams theory and the VMP approach. In the first step, considering a hypothetical pure elastic behavior for a circular beam under pure bending, a linear stress response across the cross section of the beam can be obtained, using the elastic flexural formula.

The following common assumptions taken into account when using elastic flexural formula is also true for the analysis presented here:

- cross sectional planes remain plane
- material points with the same distance from the neutral axis have the same stress
- deformations are very small and anticlastic curve is ignored

The cross section is then discretized to a finite number of elements. The center of each element is the location for representing the state of stress and strain on that element. Using the VMP method [11, 18] and the actual cyclic stress-strain curves of the material in tension and compression, results of linear elastic solution are resolved to the real elastic-plastic solution. In the VMP method, plasticity is modeled through degrading material properties at material points with plastic states of stress. Since these points are not known a priori, an iterative solution is required. The solution consists of the following steps. After the first solution (elastic solution), the value of the effective Young's modulus for each element is replaced by the Secant modulus, calculated using the projection method [11] (Figure 8). The state of stress and strain of all elements after the hypothetical elastic solution is represented by line OA, in Figure 8. Point A represents the element with maximum stress, which is located at the top of the beam. Elements at other locations of the beam cross section are represented by points lying on line OA, between O (element on neutral axis) and A (element at the top or bottom of the circular beam). To modify the behavior of any typical element like the one represented by point A with a more realistic behavior, a point on the materials stress-strain curve (blue curve in Figure 8) is found by projecting point A onto the curve and finding A'. The Modulus for the element represented

by point A is replaced by the Secant modulus of point A'. This is repeated for all elements on the cross section.

Figure 8. Projection method for updating the effective Young's (Secant) modulus for each element

Now that each element has a different modulus, the equivalent section method of composite beams is employed to construct the transformed sections and locate the new neutral axis. In this method, after the new effective Young's (Secant) modulus (E_i) for each element in the i^{th} iteration is determined, the width of the element changes in proportion to E_i/E. The second moment of the area and the location of the neutral axis will then be calculated using Equation 3, where A_i and y_i are the element's area and vertical distance from the neutral axis, respectively. All of the elements' effective Young's moduli are set to the new values and again, a hypothetical linear solution with new values of effective moduli is obtained (Figure 9). The element represented by point A in the first iteration is now represented by A_1 in Figure 8. The same updating procedure is used to adjust the effective modulus until the results of the final iteration matches the material stress-strain curve.

Figure 9. Changes in an element's shape and location of neutral axis using the method of equivalent section of composite beams

$$\text{Neutral axis translation} = \frac{\sum A_i y_i}{\sum A_i} \qquad \text{Equation 3}$$

In the case of magnesium with asymmetric behavior, the material's tensile curve is considered for elements under tension, and the material's compression curve is considered for elements under compression. The elastic-plastic solution is achieved when all of the element's stress and strain match a point on the experimentally obtained uniaxial tensile and compressive material curve. Due to the asymmetric behavior of magnesium, it is expected that the neutral axis moves up.

5. Rotating beam test and fatigue life estimation

Using hysteresis data from strain-controlled cyclic tension-compression tests on AZ31B by Albinmousa [12, 2] shown in Figure 2, peak points on these curves are selected to form tension-compression cyclic curves for this alloy (Figure 10). These tensile and compressive cyclic curves are employed as the material curves for the proposed elastic-plastic analysis.

Figure 10. AZ31 cyclic tension and cyclic compression curves

There are four different conditions that the material points on the outer surface of the specimen go through in each cycle of the RBT. Figure 11 depicts these four conditions: 1) loading from A to B, 2) unloading from B to C, 3) reverse loading from C to D, and 4) reverse unloading from D to A. In this figure, the horizontal line AC represents the neutral axis. In one full cycle of RBT, points on the surface go through positions A to D. However, in the present analysis, since the beam is fixed, the

points at the top and bottom of the beam experience the four conditions when the external load increases from zero to the maximum, back to zero, zero to the minimum, and back to zero. The points at the top of the cross section of the specimen are selected as the critical points because maximum stresses occur at these points.

Figure 11. Four conditions a material point experience in RBT that is considered in proposed analysis method: loading from A to B in tension, unloading from B to C, reverse loading in compression from C to D, and unloading from compression from D to C

According to the method described in section 4, the loading part (from A to B on Figure 11) is performed using the cyclic curves of AZ31B. To simulate the unloading and loading in reverse direction and final unloading (from B to C, C to D and D to A), the unloading curves are needed. None of the standard hardening rules can predict the hardening behavior of AZ31B, so the actual unloading and reloading curves are extracted from the data given in Figure 2 and employed [12, 2] here. Each point follows its own unique unloading and reloading curves, according to the range of strain they reach at the end of each step. Interpolation is used for cases in which the strain ranges are not available from experiments. A schematic figure of such interpolation and application of the VMP method is shown in Figure 12.

Figure 12. Applying the VMP projection method and interpolation between two experimental curves m and p, representing two different strain range, for finding the red point when the experimental results are not available for that strain range

For modeling these four steps with the proposed method, the hysteresis curves over a wide range of strain are obtained first. Using the proposed elastic-plastic analysis method, the response of material for a particular loading case under loading, unloading, reverse loading and reverse unloading is calculated using the corresponding part of the hysteresis curves. The energy method is then employed to estimate the fatigue life of the specimen, according to the plastic energy dissipated during the cycle and positive elastic energy.

6. Application of proposed method for fatigue life estimation of magnesium AZ31B under load-controlled tests

The numerical examples are for samples with the dimensions shown in Figure 3 that were stress relived, i.e, no initial residual stress. In the first example, the loading and unloading of a sample is considered. Four different moments ranging from 6-12 N·m are considered. The stress response of the sample after loading and unloading is obtained in tension and compression. Figure 13 shows the stress distribution across the circular section at the center of the specimen after loading. By increasing the load from 6 N·m to 12 N·m, the maximum stress increases by 100 MPa in both tension and compression. The neutral axis (where the curves meet the vertical axis in the figure) recedes from the centerline as the applied moment increases. Due to the lower yield value in compression at higher applied moments, elements on the compression side of the beam fail first. This results in a larger compressive portion on the cross section.

Figure 13. Stress distribution across a section of the rotating bending sample after loading; intersection of the curves with the ordinate is the location of the neutral axis

Using the stress distribution depicted in Figure 13, the force and moment balances are checked to ensure equilibrium is maintained (Table 3).

Table 3. Neutral axis translation, and force and moment balance after loading step

Item	Applied Moment			
	6 (N·m)	8 (N·m)	10(N·m)	12 (N·m)
N.A. (mm)	0.239	0.371	0.489	0.510
Force balance (N)	5.10E-13	1.20E-12	1.83E-12	-2.35E-13
Moment balance (N·m)	6.0000	7.9999	9.9999	11.9999

To find the response after unloading, the applied moment is removed. Residual stress distribution on the cross section after unloading is then calculated (Figure 14). While there was one single tensile and compressive curve for the loading step, the unloading curve for each element is different and depends on the over strain reached in the loading step. Based on the strain at the end of loading, the corresponding unloading curve is selected from the data presented in Figure 2. As the amount of applied moment increases, a peak stress develops in the tension area; as the applied moment decreases, the stress decreases and moves away from the center. The force and moment balances confirmed that residual stresses are self-balanced. At higher load levels (e.g., 12 N·m) reverse yielding occurs. Due to severe asymmetry in the cyclic behavior of AZ31B, the reverse yielding occurs at a very low compressive stress (see Figure 2). The proposed method was able to model this asymmetry and predict the reverse yielding at the higher load levels (Figure 14).

Figure 14. Residual stress distribution after unloading

With this preliminary study, the stress-strain response for a rotating bending sample is now obtained over a wider range of loads (3-12 N·m) and following one complete cycle. The hysteresis curves obtained for the most critical point of the sample (the top of the sample) at a maximum stress level are shown in Figure 15. As the applied moment increases, the hysteresis curves become nonlinear and plastic energy increases. To obtain the results for as-received samples, the method of Jahed et al. [11, 18, 20-22] in introducing the initial residual stress to the calculation was employed. At the end of loading the existing initial residual stress was added to the elastic plastic stress distribution. Therefore, the stress and strain levels at the end of loading were different from the corresponding values of stress relieved samples. Hence, different unloading and reloading curves for obtaining hysteresis in as-received material were employed as compared to the stress relieved material. This in turn led to different hysteresis, and lives for as-received and stress relieved materials at the same level of loading.

Recently, Shayegan et al. [22] developed a numerical model for obtaining the through thickness profile of residual stresses in AZ31B extrusion. Such profile is required for a complete account of initial residual stresses. However, here and as a first approximation, only the surface residual stress for the most critical point of the sample (the top of the sample) was considered.

Figure 15. Stress-strain response over one complete cycle of loading, unloading and reloading of a stress relieved sample

Using the hysteresis curves, the hysteresis energy is calculated according to the relationships shown in Figure 6. The plastic energy is calculated separately for each of the four steps (loading, unloading, reverse loading, and reverse unloading) so it is unaffected by whether a hysteresis curve is closed or overlapped. The positive elastic energy is calculated based on the maximum tensile stress of the cycle and Equation 2 is then used to calculate the fatigue life of the specimen. Total energies for stress relieved and as-received, and corresponding lives as predicted by the proposed model are presented in Table 4 and are plotted in Figure 16.

Table 4. Calculated hysteresis energy and their corresponding estimated fatigue life

Applied Moment (N·m)	Linear Stress (MPa)	Elastic plastic Stress (MPa)	Total Energy Density Stress relieved (MJ/m^3)	Total Energy Density As-received (MJ/m^3)	Estimated Life (N_f) Stress relieved	Estimated Life (N_f) As-received
3	89.09	89.09	0.090	0.026	1940530	169000000
3.5	103.94	103.94	0.123	0.044	659039	24200000
4	118.79	118.79	0.160	0.068	264067	5340000
5	148.49	143.03	0.308	0.198	32200	126900
6	178.18	171.75	0.477	0.346	9257	22342
7	207.88	194.41	0.746	0.608	3076	4930
8	237.58	209.09	1.131	1.006	1266	1593
9	267.28	218.57	1.740	1.652	565	616
10	296.97	221.48	2.179	2.124	384	399
11	326.67	233.03	3.813	3.878	159	154
12	356.37	239.02	6.126	6.376	80	75

Figure 16. Predicted S-N curves vs experiment results

A comparison of the predicted fatigue life and the experimental results are presented in the Figure 16. The predicted results, obtained using the solution proposed in this work to convert nominal stresses from the S-N curves from Figure 4 to stress amplitudes, are in a good agreement with experimental values both in trend and magnitude. It is noted that the proposed method assumes the sample to be fixed and the load to fluctuate. However, in the RBT, the load is fixed and sample rotates, which generally results in shorter lives [17]. Therefore, the predicted results are conservatively compared to the experimental results. The predicted lives for as-received samples are higher than the corresponding lives for stress relieved samples at most of the load levels, except for very high loads. Same trend was observed when experimental results of the two groups of samples were compared.

7. Conclusion

RBT of samples machined from the extrusion piece of AZ31B were tested in as-received and stress-relived conditions. A simple method was proposed to find the stress response of a load-controlled RBT for a material with asymmetric behavior. The VMP method and classical composite beam analysis were used to perform elastic-plastic analysis. As an example, RBTs of an AZ31B alloy were

considered using a dual problem that had the same load range on a fixed beam. The elastic-plastic stress response of the specimen was obtained. Using an energy method, fatigue life of the specimen was predicted and compared with the experimental results. The following is a summary of the conclusions of the study:

- Stress-relieved samples showed lower fatigue strength as compared to as-extruded samples. The residual stress induced in the extrusion process was found to be responsible for longer fatigue lives at lower stress ranges. XRD measurements showed compressive stresses as large as 43MPa at the surface of as-extruded samples.
- The VMP approach and composite beam theory were successfully applied to RBT samples to generate an elastic-plastic solution for the RBT four-point bend problem.
- The proposed model was able to find the location of the neutral axis after the application of plastic loading. The model indicated that the neutral axis moves upward to accommodate early yielding of the beam's compression side. Due to the asymmetric behavior of AZ31B, the portion of the beam cross section under compression was larger than the portion under tension.
- An energy-based fatigue model and its corresponding parameters were introduced for AZ31B. The fatigue model agrees with many available experimental results. The model was employed to predict the life of the specimen in RBT using the calculated strain energy densities obtained from elastic-plastic analysis.
- Based on material cyclic behavior, the S-N curve that includes the elastic-plastic stress of the material under a bending load was generated and compared to the RBT experimental results. The model results conservatively predicted AZ31B lives in RBT.

8. Acknowledgements

Authors would like to acknowledge the financial support of the Natural Sciences and Engineering Research Council of Canada. General Motors Research & Development Center, Warren, MI is acknowledged for making the extrusion material available through MFERD program.

9. References

[1] F. A. Mirza and D. L. Chen, "Fatigue of Mg alloys," in *Aerospace Materials Handbook*, New York, CRC Press, Taylor & Francis, 2013, pp. 647-698.

[2] J. Albinmousa, H. Jahed and S. Lambert, "Cyclic axial and cyclic torsional behavior of extruded AZ31B magnesium alloy," *Internati onal Journ al of Fatigue,* p. 1403–1416, 2011.

[3] J. Albinmousa, H. Jahed and S. Lambert, "Cyclic behavior of wrought magnesium alloy under multiaxial load," *Internati onal Journ al of Fatigue,* pp. 1127-1132, 2011.

[4] Z. Y. Nan, S. Ishihara, T. Goshima and R. Nakanishi, "Scanning Probe microscope observations of fatigue process in magnesium alloy AZ31 near the fatigue limit," *Sceripta Materiala,* vol. 50, pp. 429-234, 2004.

[5] S. Hasegawa, Y. Tsuchida, H. Yano and M. Matsui, "Evaluation of low cycle fatigue life in

AZ31 magnesium alloy," *Internati onal Journ al of Fatigue,* vol. 29, p. 1839–1845, 2007.

[6] S. M. Yin, H. J. Yang, S. X. Li, S. D. Wua and F. Yanga, "Cyclic deformation behavior of az extruded Mg 3% Al 1% Zn," *Scripta Materiala,* vol. 2008, pp. 751-754, 2008.

[7] J. Albinmousa, H. Jahed and S. Lambert, "An energy-based fatigue model for wrought magnesium alloy under multiaxial load," in *9th International conference on multiaxial fatigue and fracture*, Parma, Italy, 2010.

[8] S. H. Park, S. G. Hong, W. Bang and C. S. Lee, "Effect of anisotropy on the low-cycle fatigue behavior of rolled AZ31magnesium alloy," *Materials Science and Engineering A,* vol. 527, p. 417–423, 2010.

[9] K. Shiozawaa, J. Kitajimab, T. Kaminashic, T. Muraid and T. Takahashie, "Low cycle fatigue deformation behavior and evaluation of fatigue life on extruded magnesium alloys," *Procedia Engineering,* vol. 10, pp. 1244-1249, 2011.

[10] S. H. Kwon, K. S. Song, K. S. Shin and S. I. Kwun, "Low Cycle Fatigue Properties and an Energy-Based Approach for as-Extruded AZ31 Magnesium Alloy," *Metals and Materials International,* 2011.

[11] H. Jahed and R. A. Dubey, "An Axisymmetric Method of Elastic-Plastic Analysis Capable of Predicting Residual Stress Field," *Journal of Pressure Vessel Technology,* vol. 119, pp. 264-273, 1997.

[12] J. Albinmousa, "Multiaxial Fatigue Characterization and Modeling of AZ31B Magnesium Extrusion," University of Waterloo, Waterloo, 2011.

[13] ASM Metals Handboook, 9th ed., vol. 4, ASM International, 1989.

[14] C. Chen, T. Liu, C. LV, L. Lu and D. Luo, "Study on cyclic deformation behavior of extruded Mg-3Al-1Zn alloy," *Material Scinece and Engineering A,* vol. 539, pp. 223-229, 2012.

[15] Y. Xiong, Q. Yu and Y. Jiang, "Multiaxial fatigue of AZ31B manesium alloy," *Material Science and Engineering A,* vol. 546, pp. 119-128, 2012.

[16] H. Jahed, A. Varvani Farahani, M. Noban and I. Khalaji, "An energy-based fatigue life assessment model for various metallic materials under proportional and non-proportional loading conditions," *International Journal of Fatigue,* vol. 29, pp. 647-655, 2007.

[17] T. Hassan and Z. Liu, "On the difference of fatigue strengths from rotating bending, four-point bending, and cantilever bending tests," *International Journal of Pressure Vessels and Piping ,* pp. 19-30, 2011.

[18] H. Jahed and G. Ghanbari, "Actual unloading behavior and its significance on residual stress in machined autofrettaged tubes," *Journal of Pressure Vessel Technology,* vol. 125, pp. 321-325, 2003.

[19] R. I. Stephens, A. Fatemi, R. R. Stephens and O. Fuchs, Metal Fatigue in Engineering, John Wiley & Sons Inc., 2001.

[20] H. Jahed, B. Ahmadi, and M. Shambouli, "Re-autofrettage" *Journal of Pressure Vessels Technology,* 128 (2006), 223-226.

[21] H. Jahed, B. Farshi and M. Hosseini, "Life Prediction of Autofrettage Tubes using Actual Material Behaviour," *International Journal of Pressure vessels and piping*, Vol 83/10 (2007), pp 749-755.

[22] G. Shayegan, H. Mahmoudi-Asl, R. Ghilichi, J. Villafuerte, J. Weng, M. Guagliano, and H. Jahed, "Residual Stress Induced by Cold Spray Coating of Magnesium AZ31B Extrusion," Submitted to *Materials and Design*, JMAD-D-14-00029, 2013.

Captions for Tables

Table 1. Composition of the AZ31B extrusion

Table 2. Energy-based fatigue parameters for AZ31B

Table 3. Neutral axis translation, and force and moment balance after loading step

Table 4. Calculated hysteresis energy and their corresponding estimated fatigue life

Captions for Figures

Figure 1. Typical cyclic behaviour of magnesium alloy AZ31B extrusion within one cycle of loading [2]

Figure 2. Hysteresis curves of AZ31B under cyclic uniaxial loading; a) 0.2%-0.6% and b) 0.7%-2% [12]

Figure 3: Round rotating bending specimens of AZ31B

Figure 4. S-N curves of as-received and stress-relieved specimens of AZ31B

Figure 5. Total energy-life curve for AZ31B

Figure 6. Positive elastic and plastic energy in a hysteresis curve

Figure 7. Schematic of the loading of a specimen in RBT

Figure 8. Projection method for updating the effective Young's (Secant) modulus for each element

Figure 9. Changes in an element's shape and location of neutral axis using the method of equivalent section of composite beams

Figure 10. AZ31 cyclic tension and cyclic compression curves

Figure 11. Four conditions a material point experience in RBT that is considered in proposed analysis method: loading from A to B in tension, unloading from B to C, reverse loading in compression from C to D, and unloading from compression from D to C

Figure 12. Applying the VMP projection method and interpolation between two experimental curves m and p, representing two different strain range, for finding the red point when the experimental results are not available for that strain range

Figure 13. Stress distribution across a section of the rotating bending sample after loading; intersection of the curves with the ordinate is the location of the neutral axis

Figure 14. Residual stress distribution after unloading

Figure 15. Stress-strain response over one complete cycle of loading, unloading and reloading of a stress relieved sample

Figure 16. Predicted S-N curves vs experiment results

Figure 1

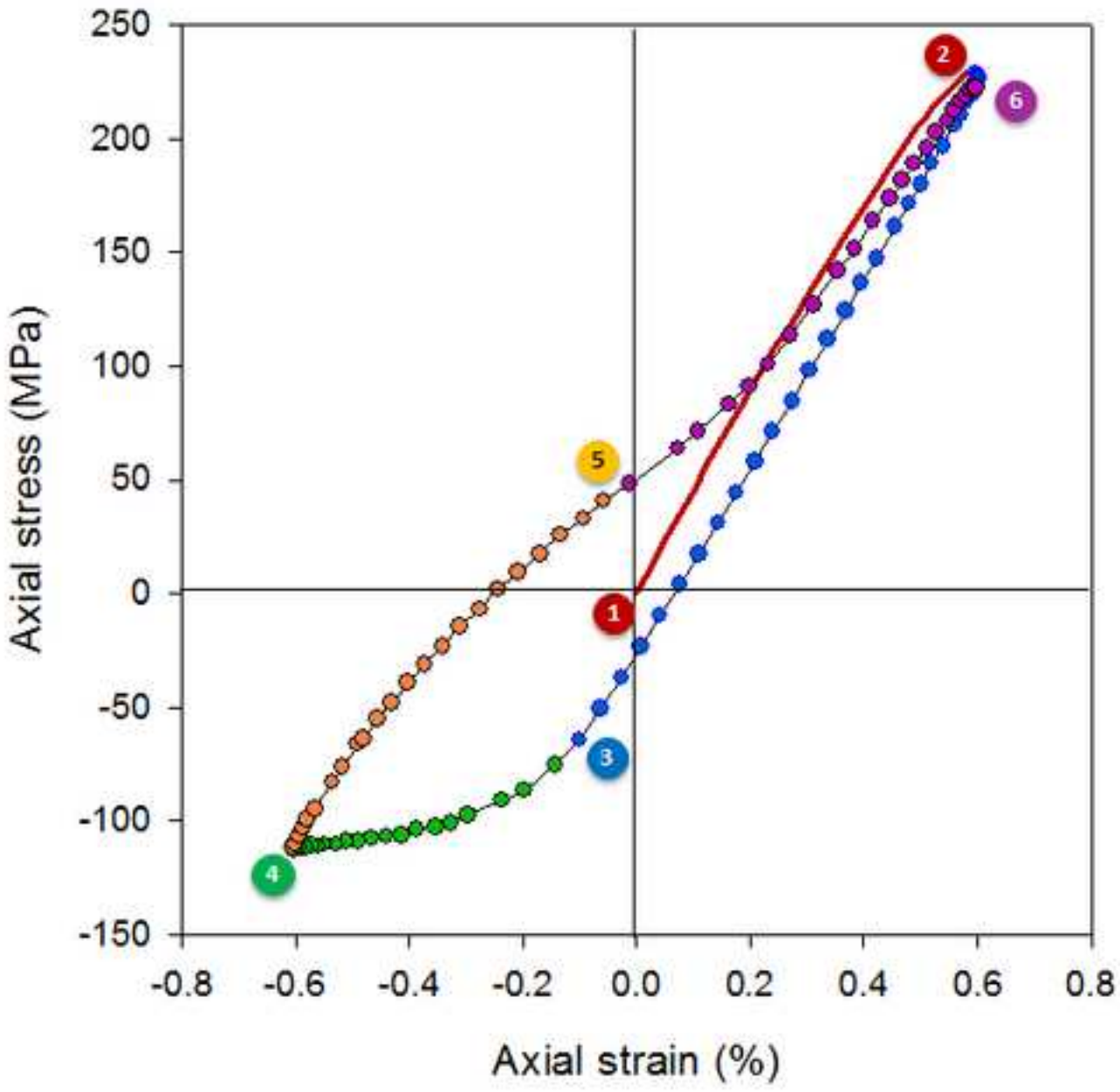

Figure 2

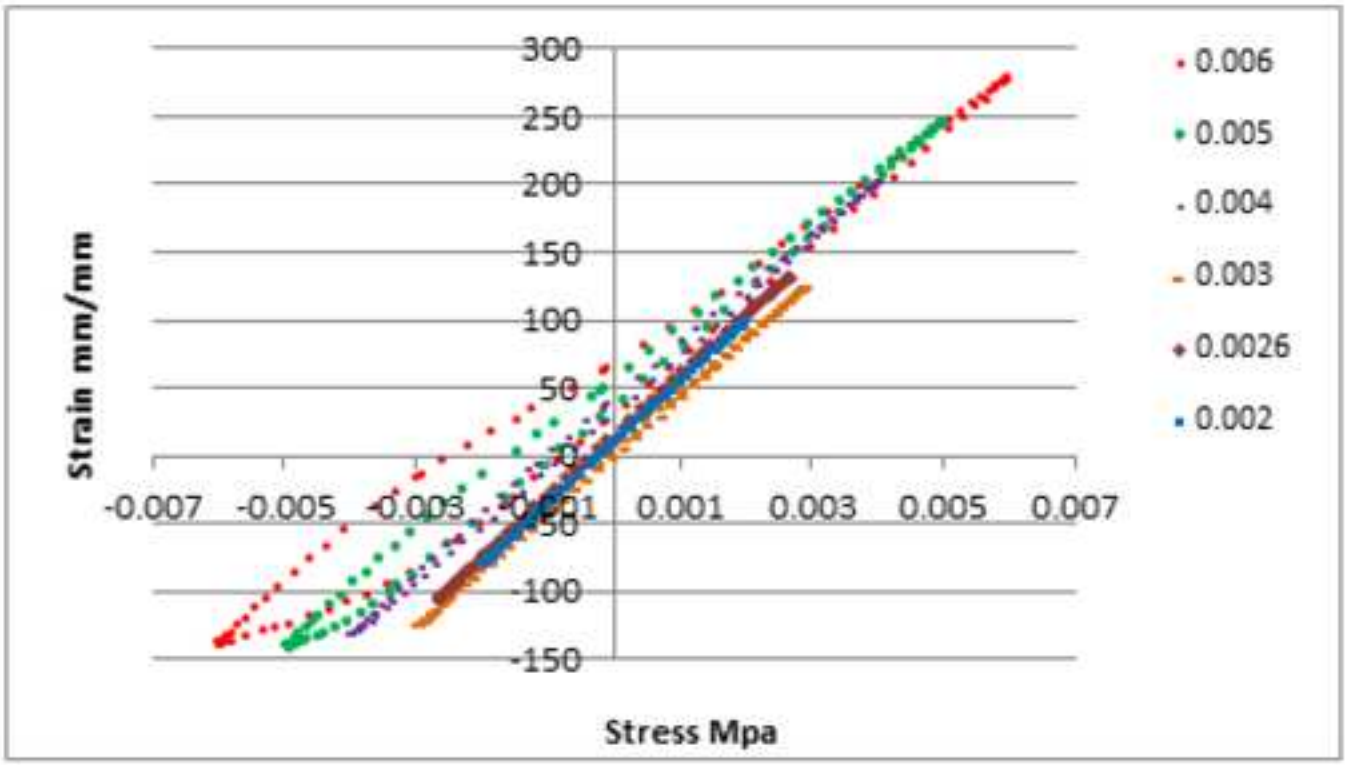

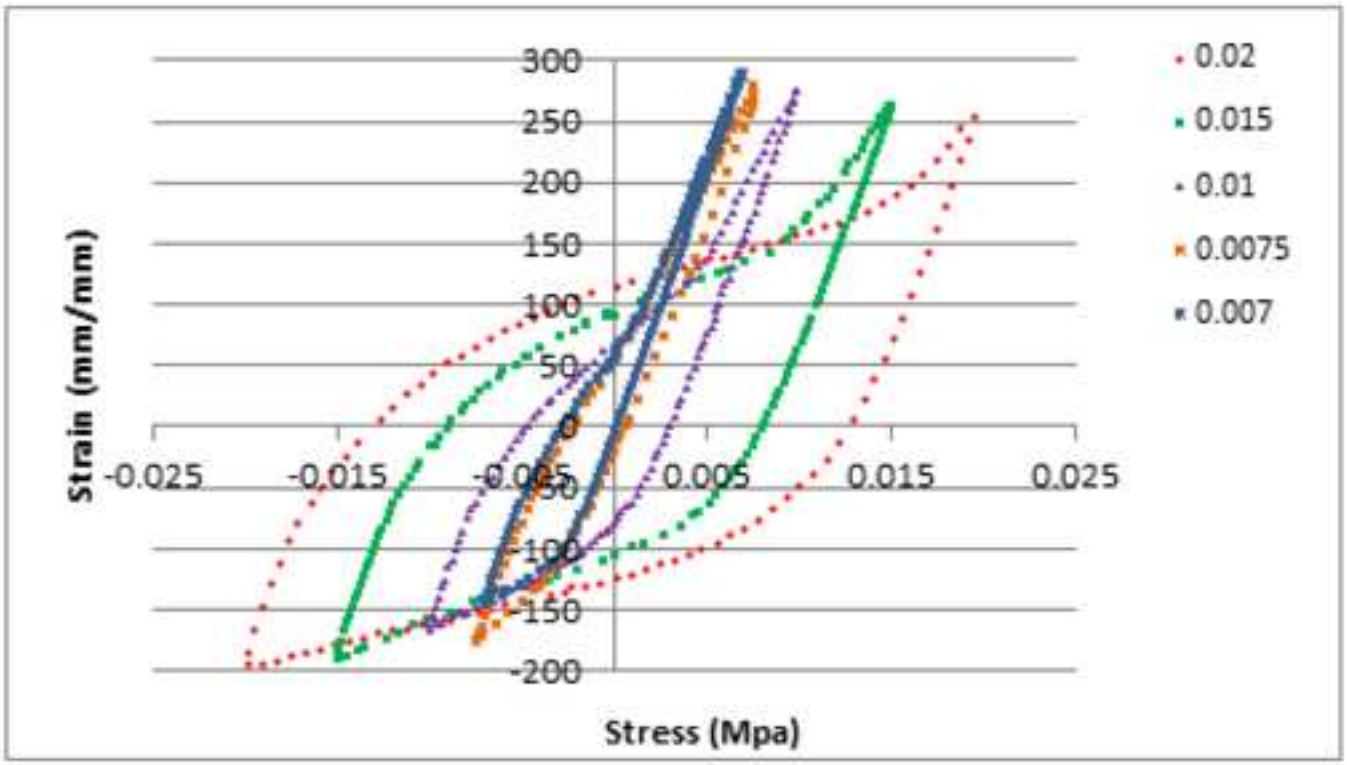

Figure 3

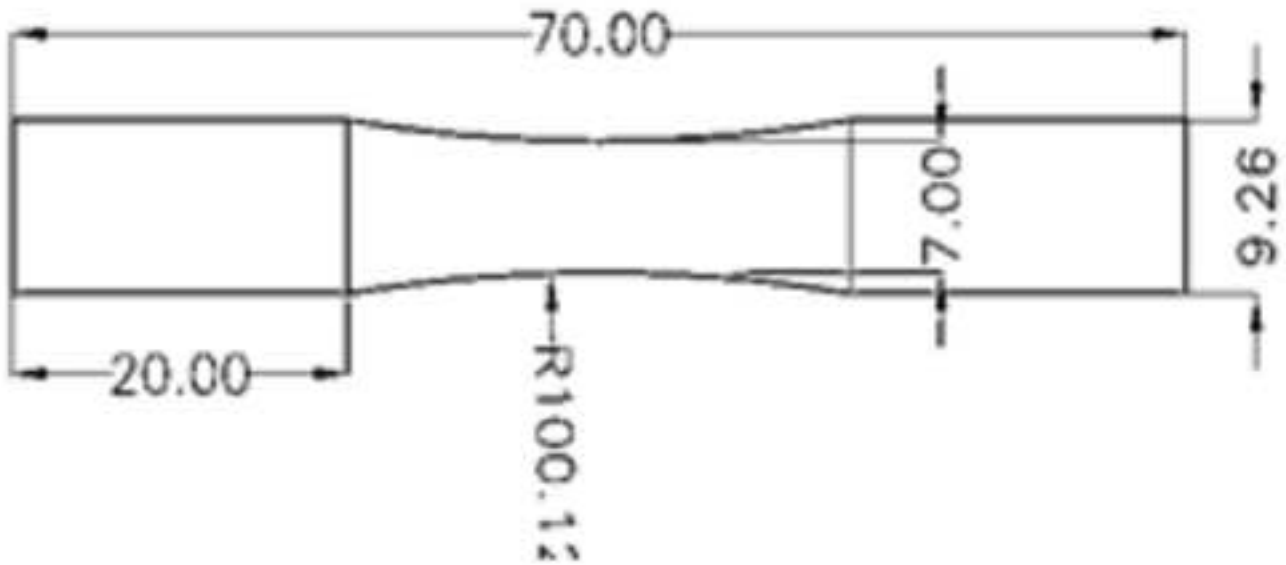

Figure 4

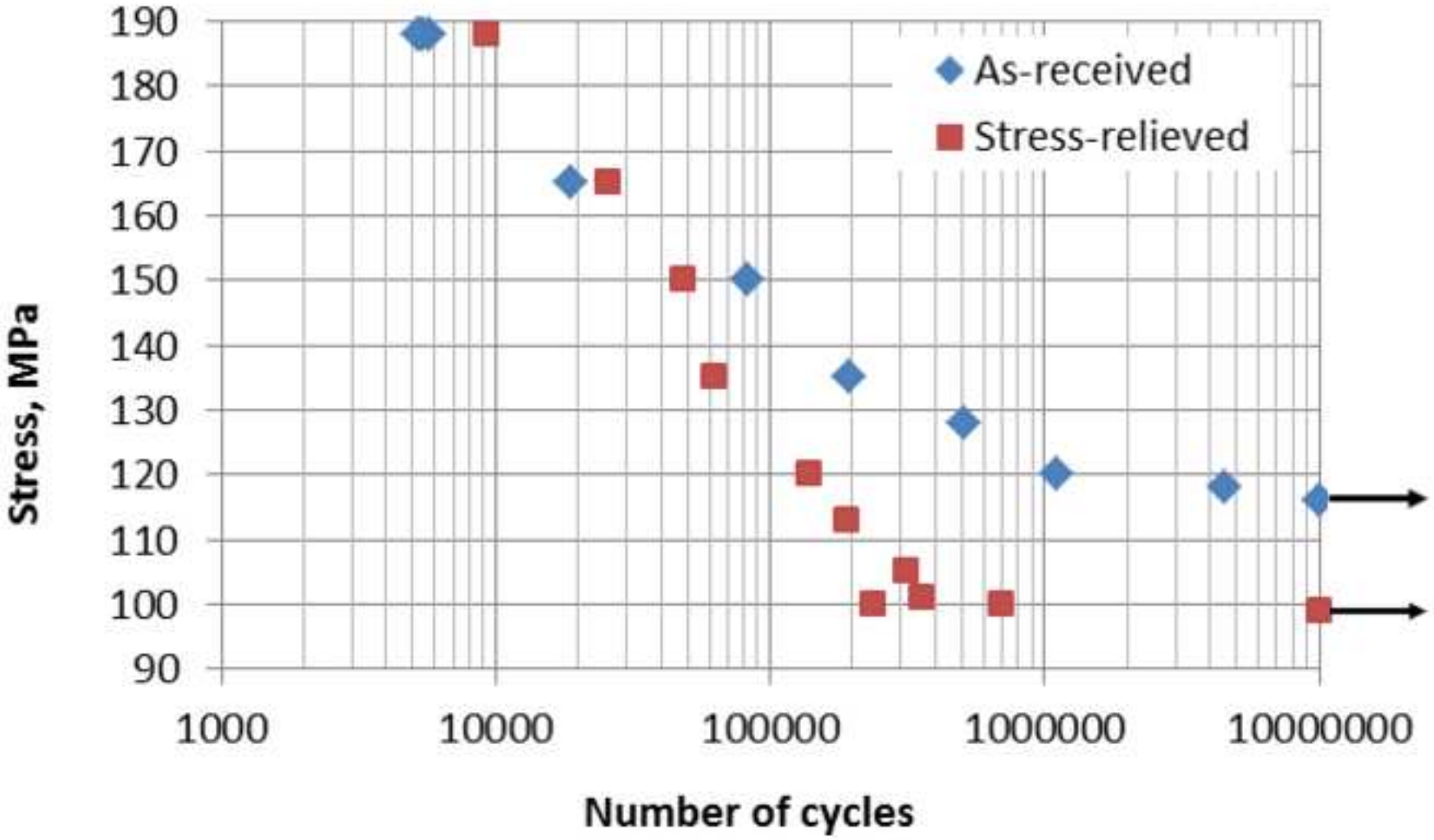

Figure 5

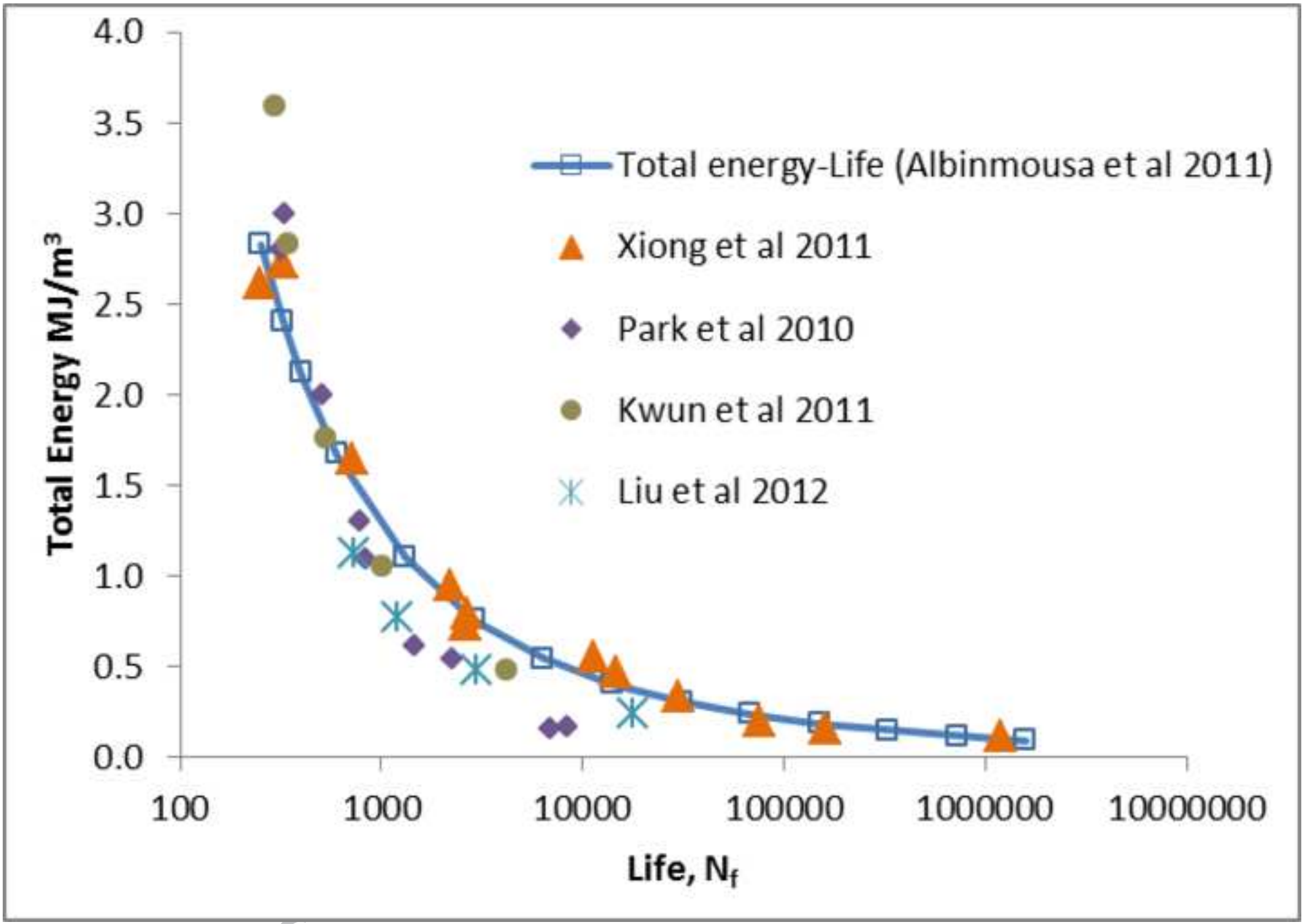

Figure 6

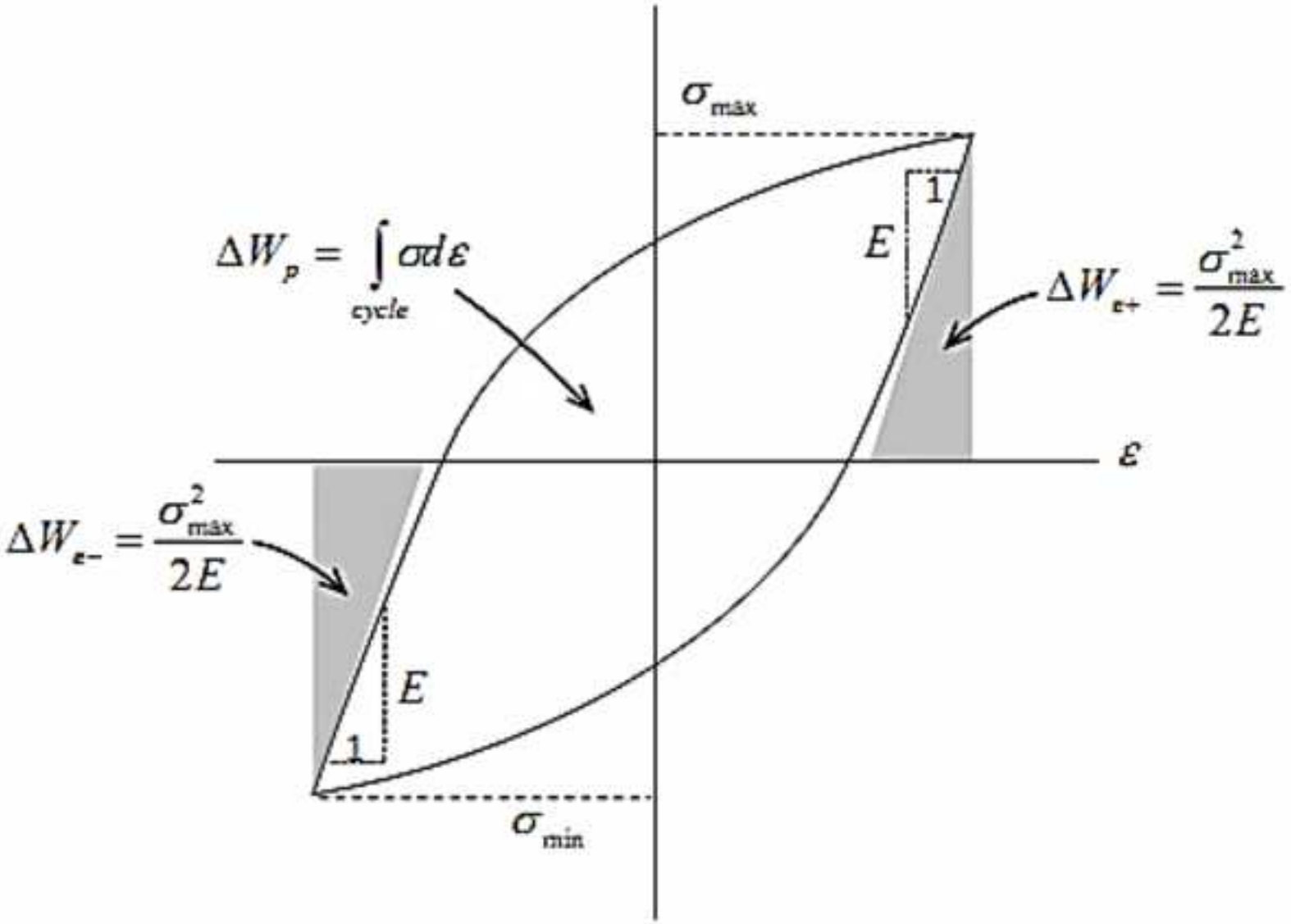

Figure 7

Figure 8

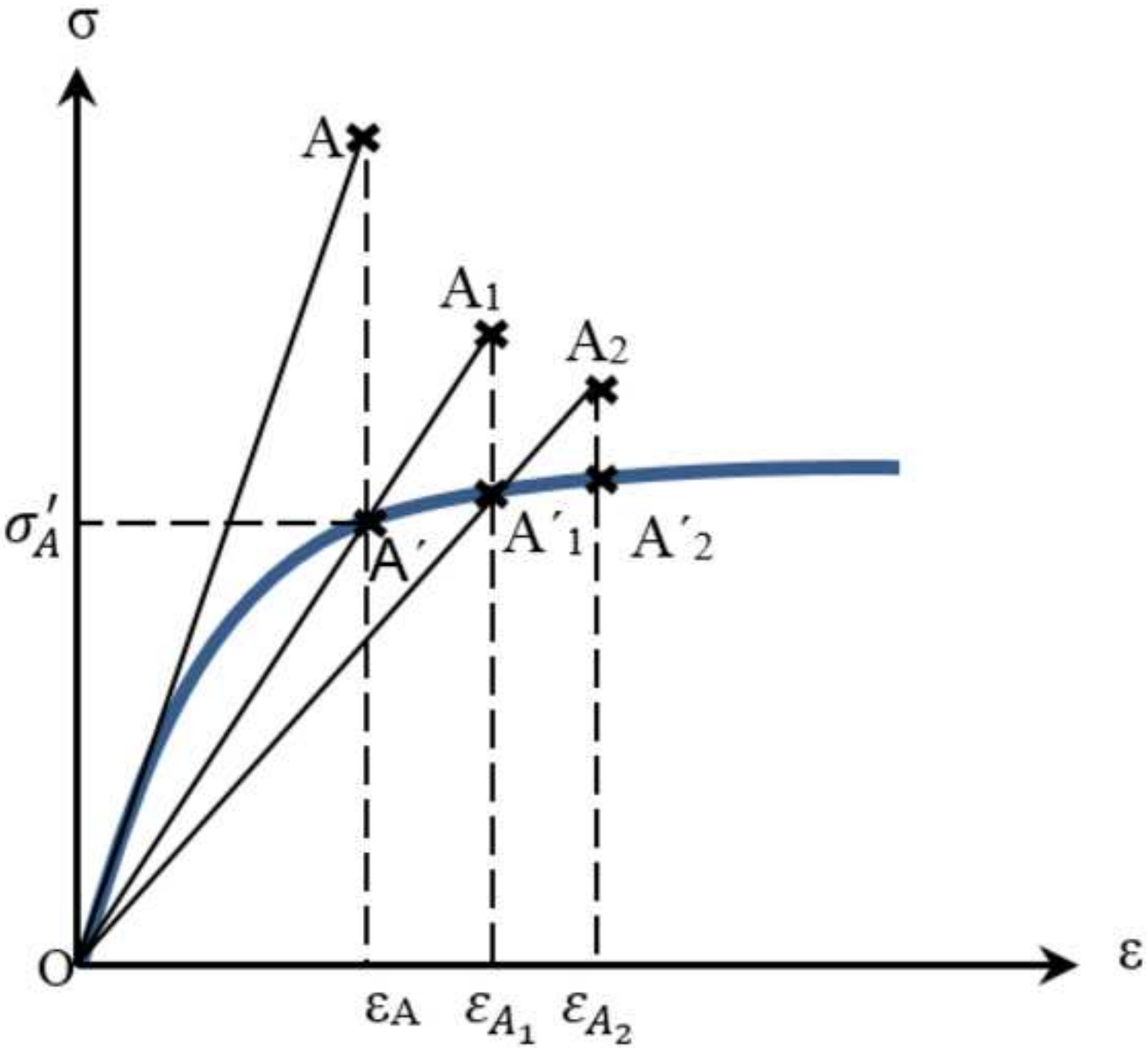

Figure 9

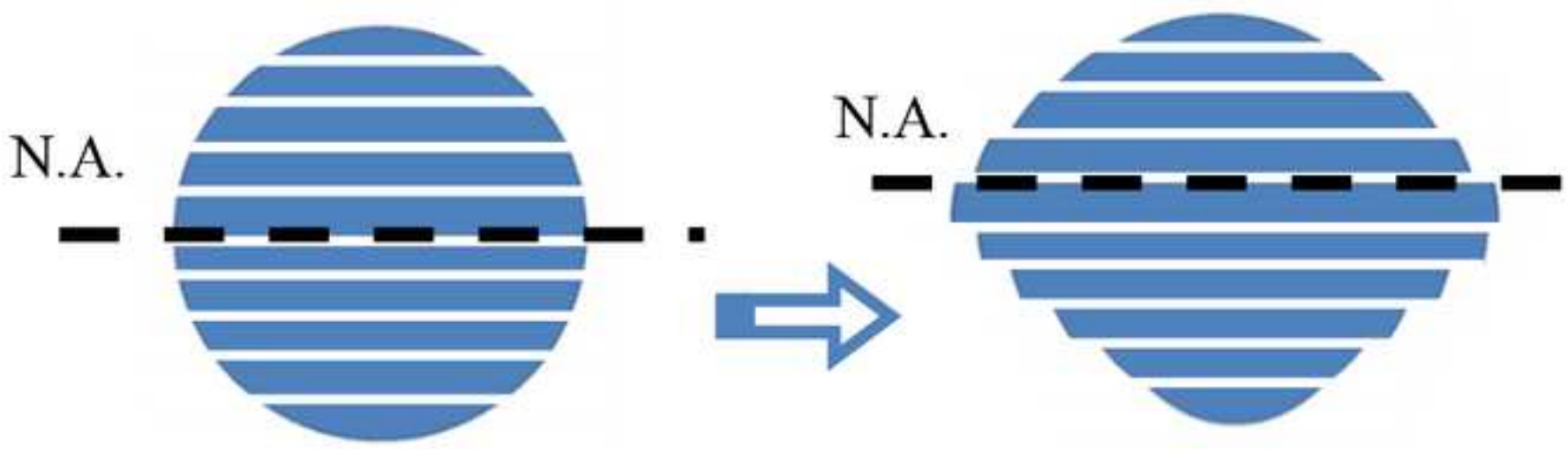

Figure 10

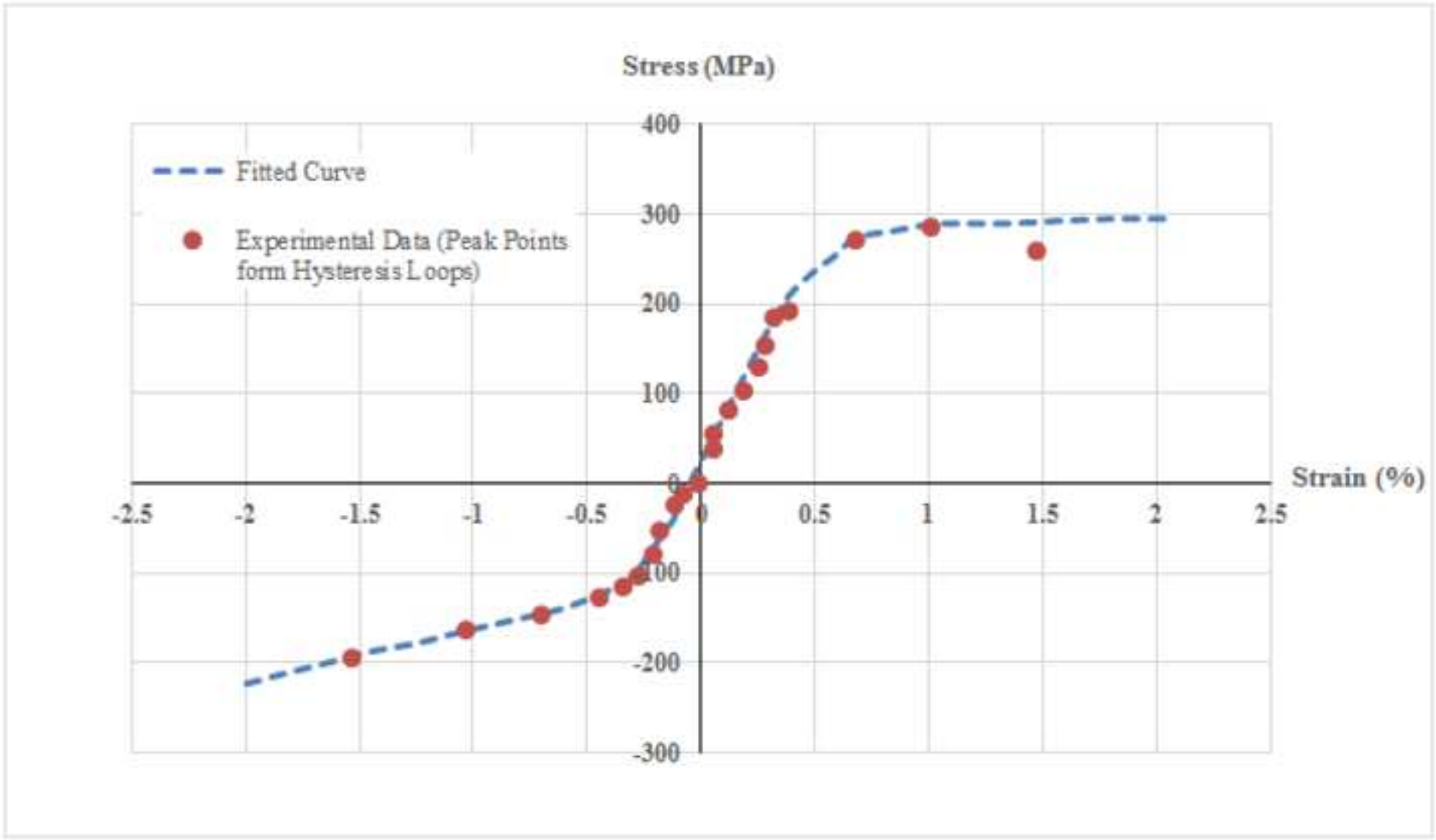

Figure 11

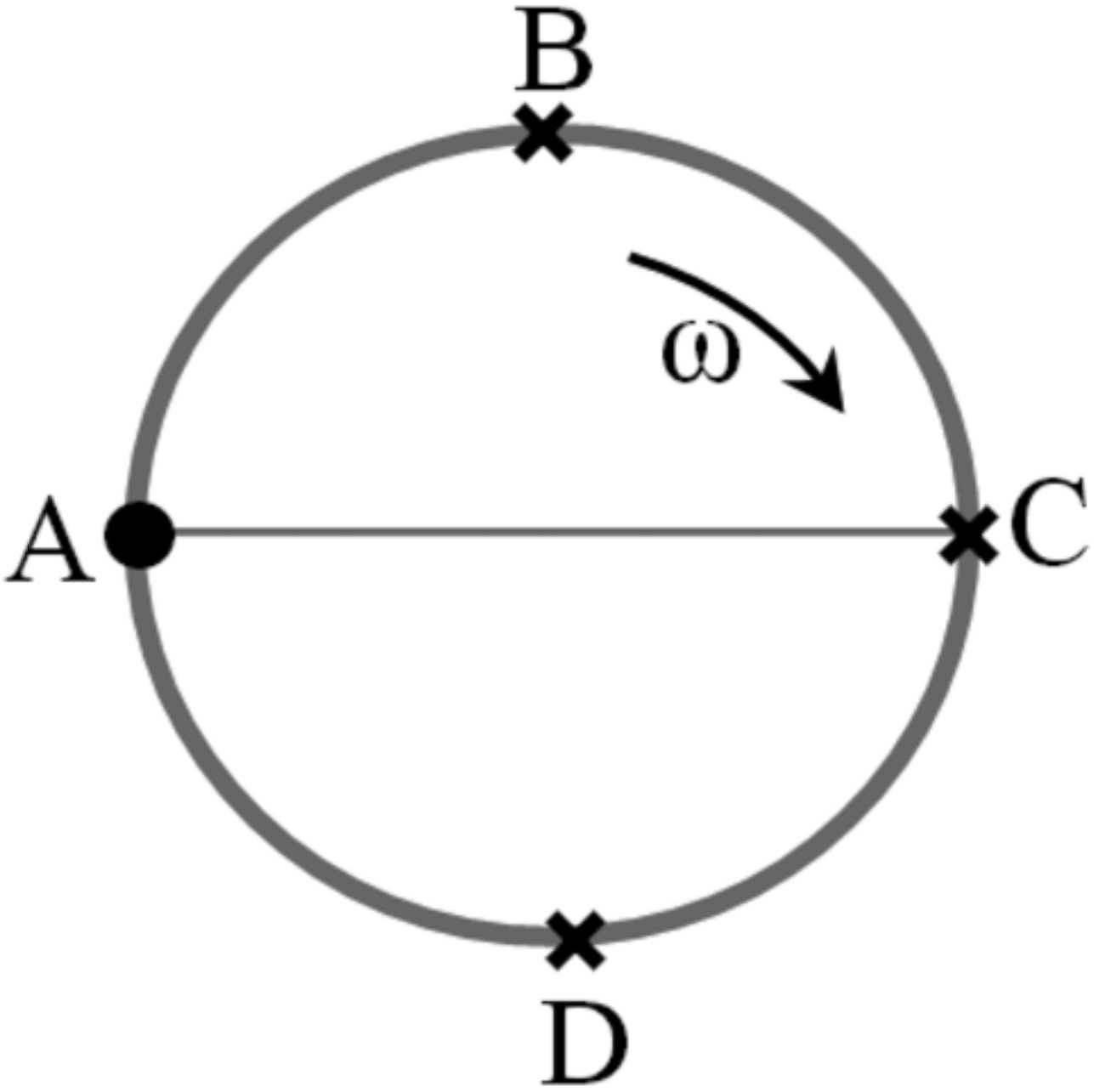

Figure 12

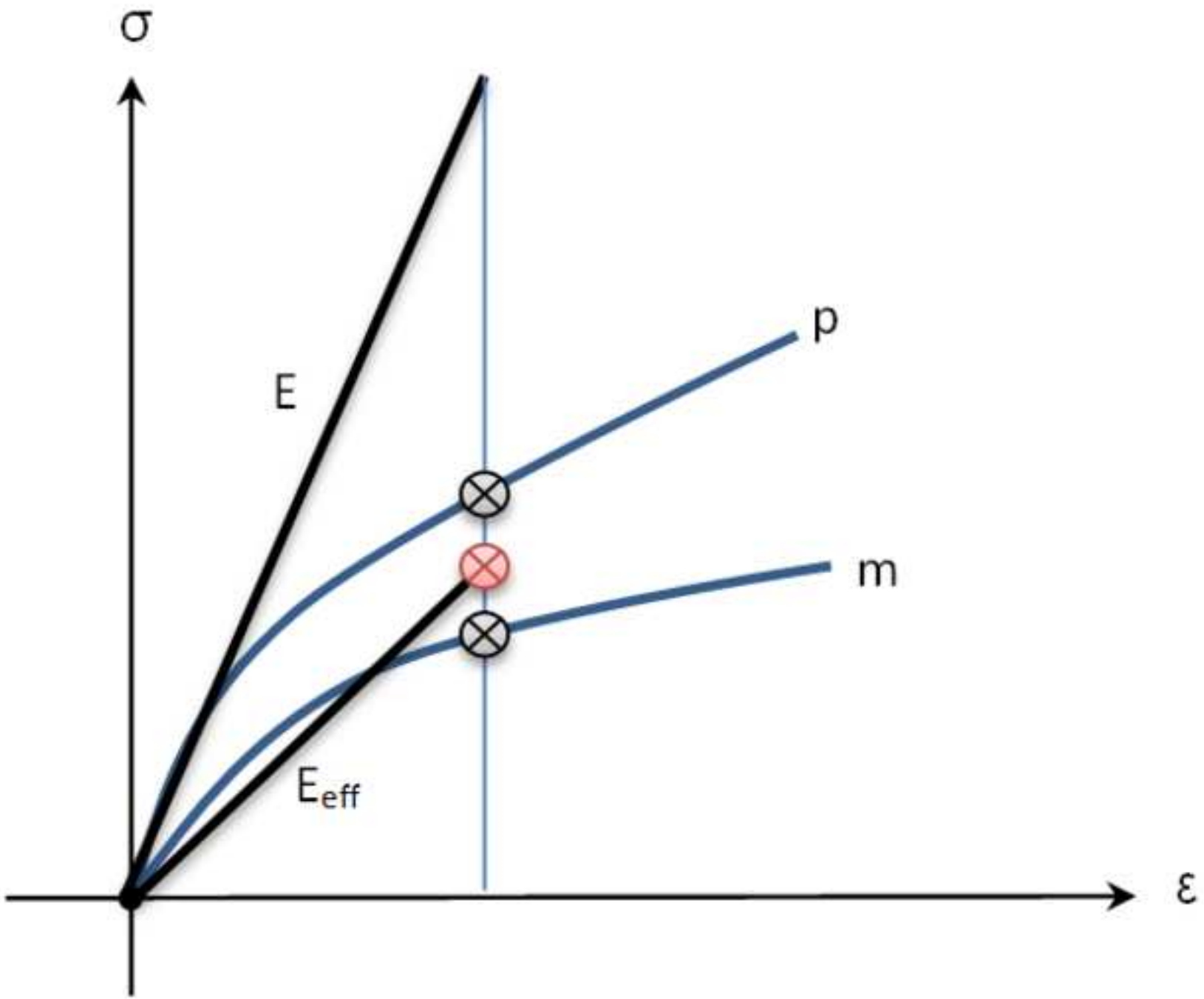

Figure 13

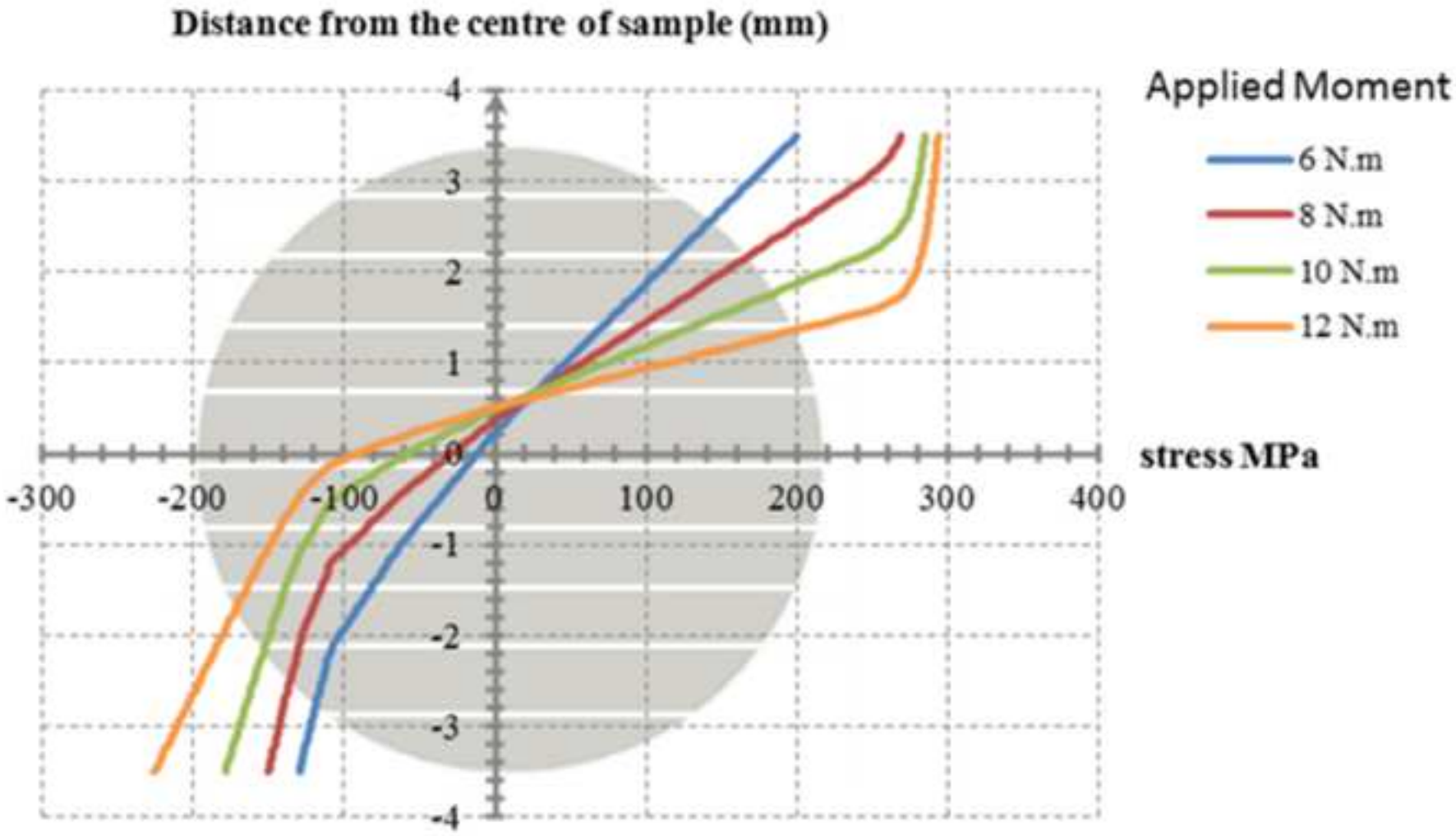

Figure 14

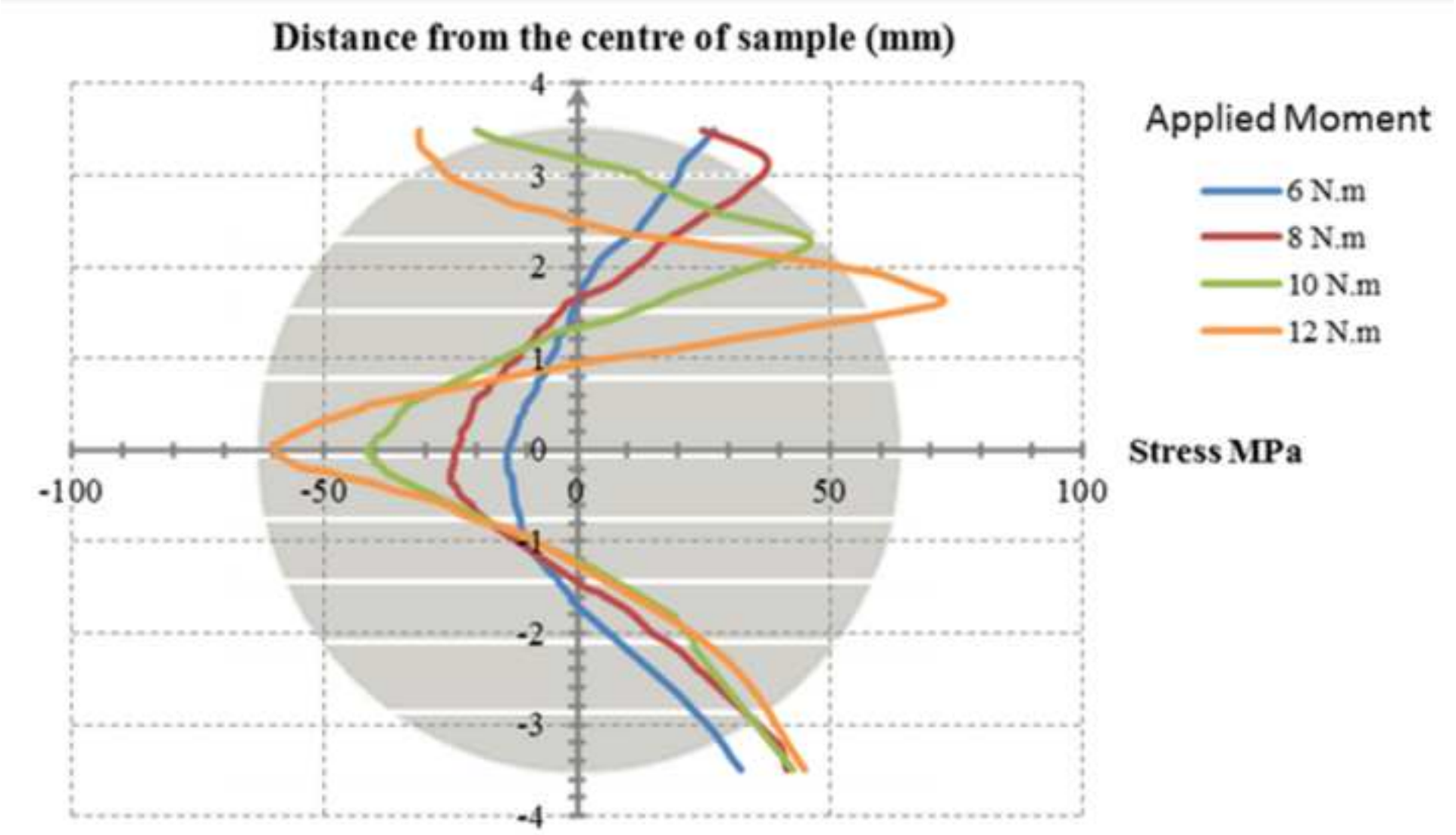

Figure 15

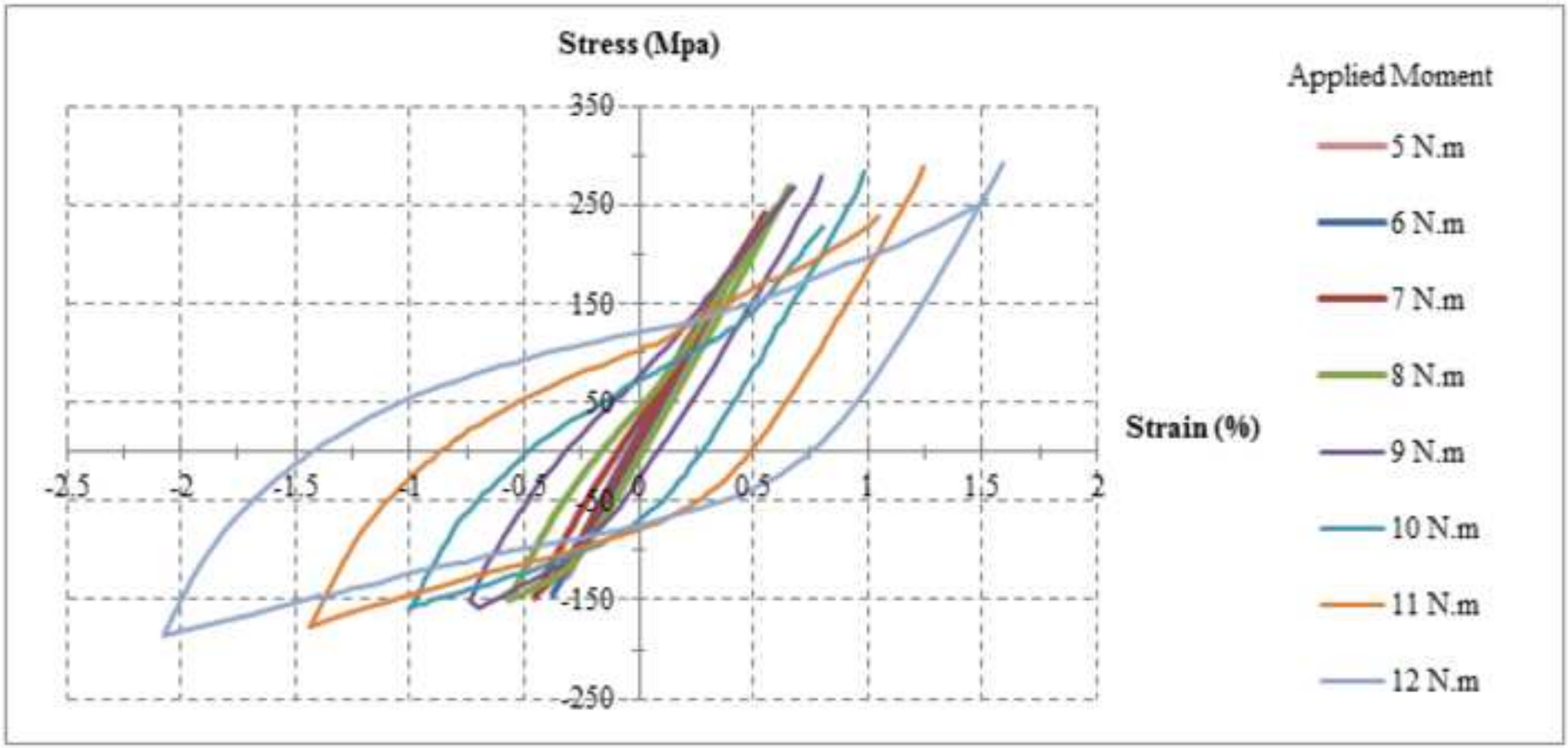

Figure 16

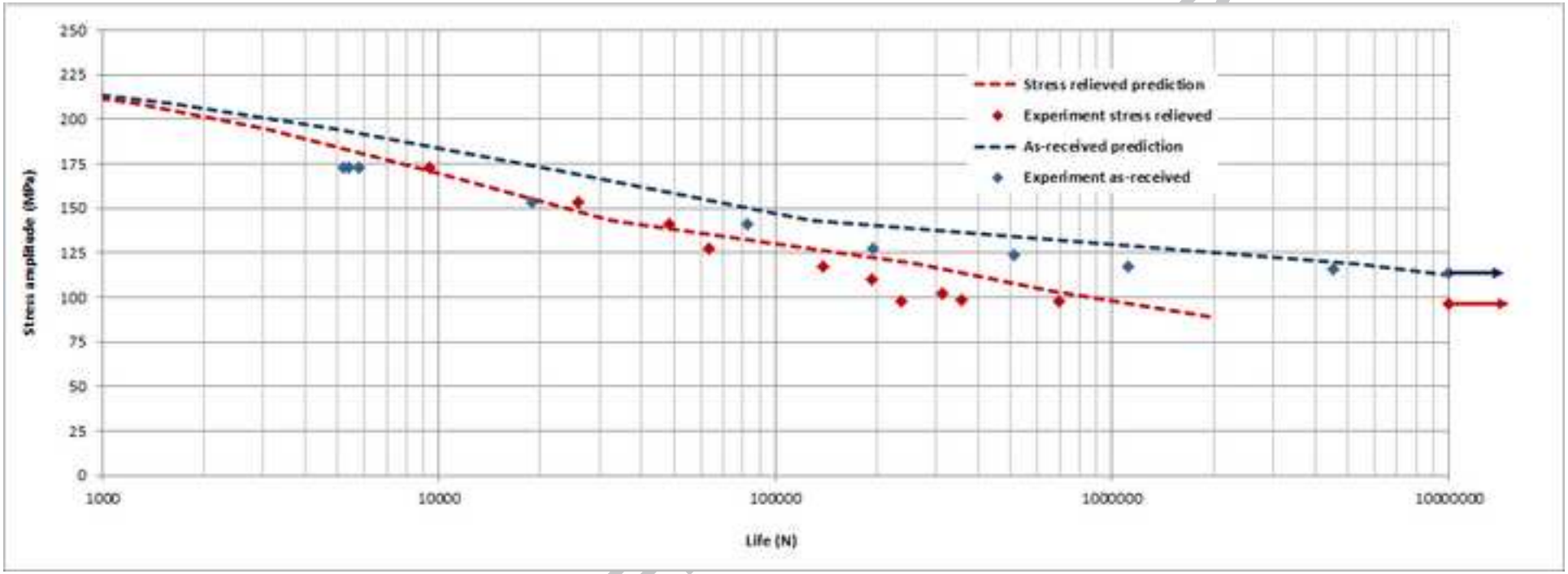

Table 1. Composition of the AZ31B extrusion

Al	Mn	Zn	Fe	Ni	Cu
3.10	0.54	1.05	0.0035	0.0007	0.0008

Table 2. Energy-based fatigue parameters for AZ31B

Elastic Part- high cycle	E_f	**5**
	b	**-0.278**
Plastic Part- low cycle	W_f	**190**
	c	**-0.848**

Table 3. Neutral axis translation, and force and moment balance after loading step

Item	**Applied Moment**			
	6 (N·m)	**8 (N·m)**	**10(N·m)**	**12 (N·m)**
N.A. (mm)	0.239	0.371	0.489	0.510
Force balance (N)	5.10E-13	1.20E-12	1.83E-12	-2.35E-13
Moment balance (N·m)	6.0000	7.9999	9.9999	11.9999

Table 4. Calculated hysteresis energy and their corresponding estimated fatigue life

Applied Moment (N·m)	**Linear Stress (MPa)**	**Elastic plastic Stress (MPa)**	**Total Energy Density Stress relieved (MJ/m^3)**	**Total Energy Density As-received (MJ/m^3)**	**Estimated Life (N_f) Stress relieved**	**Estimated Life (N_f) As-received**
3	89.09	89.09	0.090	0.026	1940530	169000000
3.5	103.94	103.94	0.123	0.044	659039	24200000
4	118.79	118.79	0.160	0.068	264067	5340000
5	148.49	143.03	0.308	0.198	32200	126900
6	178.18	171.75	0.477	0.346	9257	22342
7	207.88	194.41	0.746	0.608	3076	4930
8	237.58	209.09	1.131	1.006	1266	1593
9	267.28	218.57	1.740	1.652	565	616
10	296.97	221.48	2.179	2.124	384	399
11	326.67	233.03	3.813	3.878	159	154
12	356.37	239.02	6.126	6.376	80	75

An Asymmetric Elastic-Plastic Analysis of the Load-Controlled Rotating Bending Test and Its Application in the Fatigue Life Estimation of Wrought Magnesium AZ31B

Highlights

- As-extruded and stress-relived samples of AZ31B are tested on a RBM.
- Elastic-plastic method of analysis that considers yield and hardening asymmetry of wrought magnesium alloys is proposed.
- Stress distribution, cyclic hysteresises and strain energy density in RBT of AZ31B are obtained.
- Using an energy-life model, fatigue life of AZ31B in RBT is predicted.
- The model S-N results are conservatively predicting AZ31B lives in RBT.